AFM Resolves Dynamic Effects of Ethambutol on Nanomechanics and Nanostructures of Single Dividing Mycobacterium Cells

Yangzhe Wu[1,2], Ronald C. Sims[1], Anhong Zhou[1,*]

[1]Department of Biological Engineering, Utah State University, Logan, UT 84322, USA
[2]Department of Microbiology and Immunology, College of Medicine, University of Illinois at Chicago, Chicago, IL 60612 USA
Tel: (435)79792863; Fax: (435)7970148; Email: Anhong.Zhou@usu.edu

ABSTRACT

Dynamic nanomechanics and nanostructures of dividing and anti-mycobacterial drug treated mycobacterium are yet to fully elucidate. Atomic force microscopy (AFM) is a promising nanotechnology to characterize such dynamic properties, especially at the single cell level. In this work, single dividing mycobacterium JLS (M.JLS) before and after anti-mycobacterial drug (ethambutol, EMB) treatment was *in situ* quantitatively characterized, suggesting that nanomechanics would be referred as a sensitive indicator for evaluating efficacy of antimycobacterial drugs. Dynamic evidences on contractile ring and septal furrow of dividing M. JLS implied that inhibition of contractile ring formation would be a crucial process for EMB to disturb M.JLS division. These results facilitated further explaining the regulation mechanism of the contractile ring as well as nanomechanical roles associated with mycobacterial division or drug treatment.

Keywords: atomic force microscopy, mycobacterium JLS, cell division, anti-mycobacterial drug

1 INTRODUCTION

M. Tuberculosis causes more human deaths worldwide than any other pathogen. It has been intensively studied because it infects about one-third of the world's population and causes about two million deaths annually [1]. Difficulties in treating *M. Tuberculosis* are mainly due to two factors: 1) the rigid, thick cell wall with low permeability that is a common feature of *mycobacterium*; and 2) increasing drug resistance. The common core of the mycobacterial cell envelope consists of an outer layer of mycolic acids covalently bound to peptidoglycan via the arabinogalactan (mAGP complex) [2]. The biosynthesis of arabinogalactan, which is a bridge component of the cell wall skeleton, can be inhibited by an anti-mycobacterial drug, ethambutol (EMB) [3, 4], which disrupts the arabinosyltransferase and likely leads to a loss of cell wall integrity. Therefore, it is reasonable to hypothesize that EMB treatment would suppress cell division by inhibiting biosynthesis of cell wall components (e.g. reducing arabinogalactan contents) and eventually alter biophysical properties of mycobacterium cells, including cell wall adhesion and stiffness.

To fully illuminate the dynamic influences of EMB exposure on mycobacteria at the single cell level, most important thing is to further reveal the alterations of mycobacterial skeleton structures induced by EMB, because the skeleton structures play crucial roles in the regulations of mycobacterial division, gene expression, cell shape maintenance, motility, and protection of cell membrane rupture triggered by turgor pressure [5]. An effective approach is to quantify the alterations of nanomechanical property as it is closely correlated with cytoskeletal changes. Currently, nanomechanics have been shown to be a promising, sensitive, and quantitative indicator of alterations of both inner skeleton structures and cell surface adhesion property [5]. Thus, nanomechanical detections can provide quantitative information about the dynamics of skeletal organization of mycobacteria in the division process with presence of anti-mycobacterial drug, which could further understanding of skeletal regulation and response mechanism in the context of mycobacterial division and anti-mycobacterial drug treatment. Atomic force microscopy (AFM), a powerful nanotechnology that is capable of imaging cell membrane surface nanostructures [6] and measuring nanomechanics [5] of single cells in their native states, has been extensively applied to detect *mycobacterium* cells [3, 4].

In the present work, AFM was employed to quantitatively measure nanomechanical alterations of EMB treated and untreated mycobacteria. In this work, *mycobacterium* sp. strain JLS (*M. JLS*), a non-pathogenic *mycobacterium* isolated from creosote-contaminated soil [7] that exhibits polycyclic aromatic hydrocarbon-degrading activities in bioremediation, bioaugmentation, and biodegradation applications [7, 8], is used as a model mycobacterial cell line. Although the biosynthesis pathways of the *M. JLS* cell wall have not been fully elucidated, *M. JLS*'s ease of use and general biosafety profile make it an excellent model organism for investigating the interaction of anti-mycobacterial drugs and mycobacteria that may lead to the design and development of new drugs to treat mycobacteria-involved diseases (such as *tuberculosis*).

2 MATERIALS AND METHODS

The *mycobacterium* sp. strain *JLS* (*M. JLS*) was obtained from Dr. Ronald Sims' and Dr. Charles Miller's

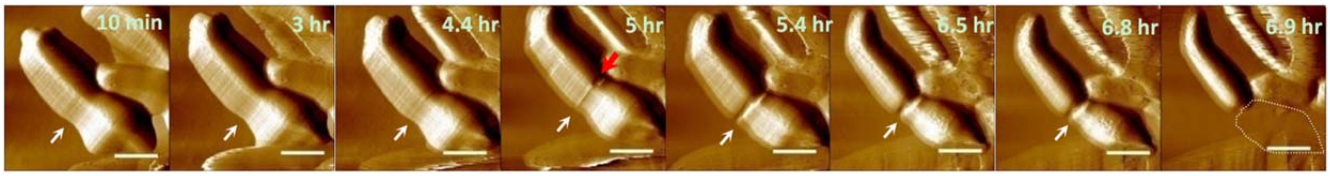

Figure 1. *In situ* consecutive observations of asymmetric dividing *M. JLS* acquired by contact mode AFM in culture medium. White arrows indicate formation of the contractile ring, and the red arrow (5 hr) shows the location of cell wall split and depression, followed by the formation of two offspring (5.4 hr). At 6.9 hr, one of the newly formed offspring was pushed away by the AFM tip (dashed white curve). Scale bar: 1 μm.

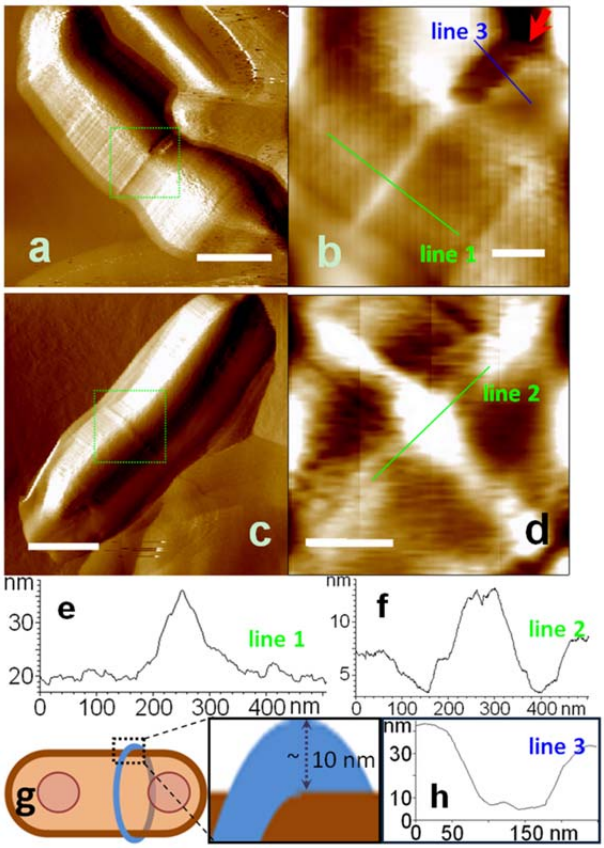

Figure 2. Visualization of contractile ring in dividing *M. JLS*. **(a)** and **(c)** are two single bacteria; **(b)** and **(d)** show enlarged topographical views corresponding to the green square frames in **(a)** and **(c)** respectively. The red arrow **(b)** indicates initiation of cell wall splitting and septal furrow generating. Representative cross-sections taken along the green and blue lines 1-3 in **(b)** and **(d)** are displayed in **(e)**, **(f)** and **(h)**, respectively. **(g)** A schematic drawing of the formed contractile ring (blue ring) of dividing *M. JLS*, approximately 10 nm in height. Scale bar: 1 μm **(a, c)**, 200 nm **(b, d)**.

laboratories at the Department of Biological Engineering at Utah State University (Logan, Utah). The cells were cultured in LB broth composed of yeast extract, peptone from casein, and sodium chloride (mass ratio, 1:2:1) at room temperature by the normal shaking method. In our experiments, 10 μg/ml of EMB dissolved in LB broth medium was used to treat *M. JLS* by referring to the minimal inhibitory concentration (MIC) of EMB to *Mycobacterium bovis BCG* [4] and to other *Mycobacterium* strains [9]. For comparison, two higher concentrations, 25 μg/ml and 50 μg/ml, were also used. All AFM measurements were conducted in LB broth medium at ambient room temperature.

Contact mode AFM (PicoPlus, Agilent Technologies, U.S.A) was applied for imaging and mechanical measurements. Values of adhesion force (detachment force between AFM tip and cell wall during probe retraction) were extracted from deflection (nm) vs. distance (nm) curves using Scanning Probe Image Processor (SPIP) software (Image Metrology, Denmark). To statistically assess nanomechanical properties, data were analyzed using one-way ANOVA and reported as mean±SE (standard error of mean). The data used to graph histograms or maps were measured from the whole cell wall, and OriginPro 7.5 (OriginLab Corp., USA) was used to plot histograms. The 256-color maps of adhesion force or cell elasticity were graphed by Matlab program version R2009a (MathWorks, Inc.) as previously described [10].

3 EXPERIMENTAL RESULTS

3.1 Real-time Visualizing division of M. JLS

Dynamic variations in cell wall structures associated with cell division of single *M.JLS* were first visualized by contact mode AFM (**Fig. 1**), which recorded in real-time the formation of the contractile ring (white arrows in **Fig. 1**), the progression of cell wall splitting and depressing (red arrow at 5 hours), and the formation of the septal furrow. The visualization of two offspring of unequal size, a larger mother cell and a smaller daughter cell (5.4 hours), clearly revealed the asymmetric division of *M. JLS*. Interestingly, it demonstrated that the newly formed daughter cell could be pushed away by the AFM tip (6.9 hours), which was likely due to synergetic effects of lateral force applied by the contact mode AFM tip and reduced adhesion of the newly formed daughter cell during the dividing process.

During the course of cell division, it was interesting to record the dynamic emergence of the contractile ring (or cell wall furrow ring), illustrating that the contractile ring protrudes out of the cell wall surface (**Fig. 2a-2d**). This was confirmed by measurement of their heights (**Fig. 2e**, **2f**):

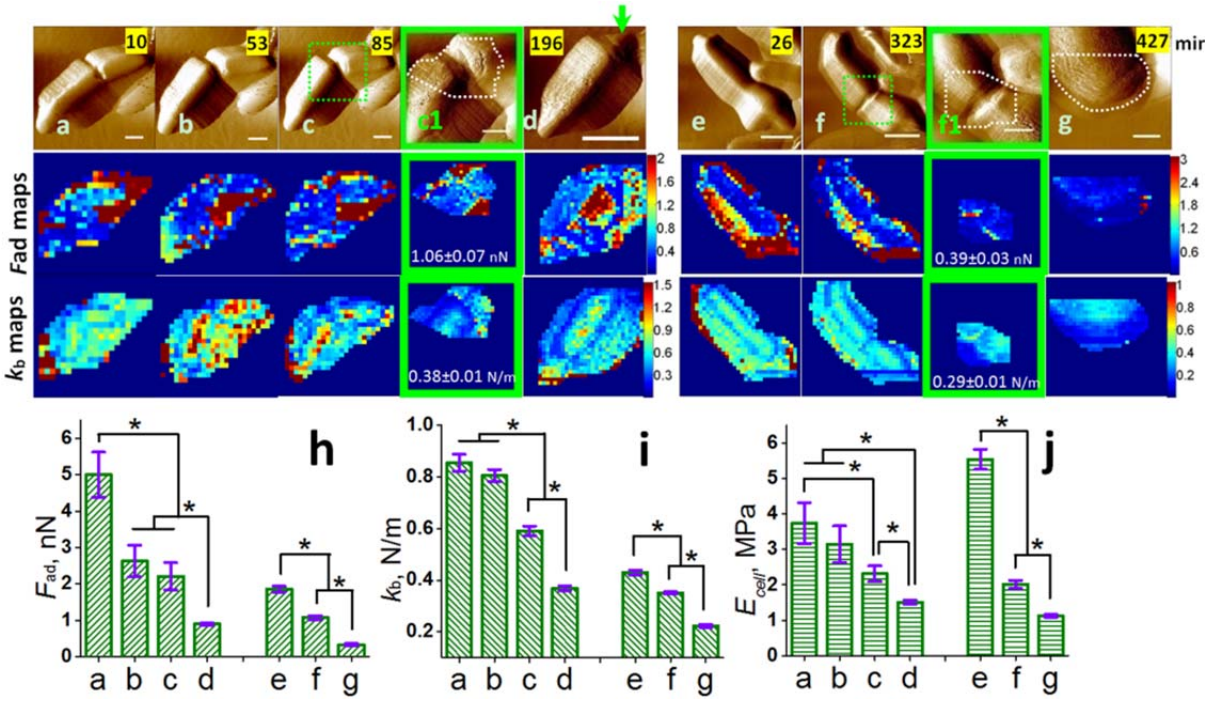

Figure 3. *In situ* tracking observations and measurements of dividing *M. JLS* using contact mode AFM in culture medium. Images in row 1 are deflection images, showing two dividing bacterial cells (**a**; **e**); the images highlighted by green frames **(c1, f1)** are enlarged views of the septal regions of **(c)** and **(f)**, respectively. Maps of adhesion force (F_{ad}, nN) and spring constant (k_b, N/m) measured at each time point are correspondingly shown under each image (rows 2, 3); and force maps of columns 4 and 8 were measured from the regions highlighted by white dotted curves in **(c1)** and **(f1)**, respectively, showing a lower adhesion force and cell elasticity at the septal furrow than the rest of cell wall (statistical data marked on each image). **(h-j)** Statistical comparison of F_{ad}, k_b, and Young's modulus (E_{cell}, MPa) shows significant decreases with the progression of cell division. * Significant difference, $P < 0.01$. Each time point has a different datum point, 'n', which ranges from ~200 to ~700. Scale bar: 1 µm **(a-f)**, 400 nm **(c1, f1)**, 200 nm **(g)**.

13.08 ±0.48 nm and 7.93±0.54 nm for contractile ring in Fig. 2b and Fig. 2d, respectively. Statistical analysis of these contractile ring based on multiple cells estimated that the contractile ring of dividing *M. JLS* protrudes outward from cell wall approximately 10 nm (**Fig. 2g**). **Figures 2a** and **2b** suggest simultaneous cell wall splitting and formation of the septal furrow, which occurred prior to formation of daughter cells. Measurements showed the septal furrow to be 26.19±0.98 nm in depression depth and 130.69±2.03 nm in Full Width at Half Maximum (**Fig. 2h**).

3.2 Nanomechanics of dividing and EMB treated M. JLS

To assess dynamic variations in cell nanomechanics of dividing *M. JLS*, cell wall surface adhesion force (*F*ad), cell wall spring constant (k_b), and Young's modulus (E_{cell}) were obtained from the force-distance curves (**Fig. 3**). Statistical analysis quantified that these three parameters (*F*ad, k_b, E_{cell}) were down-regulated in the process of cell division (**Fig. 3h-3j**). On the other hand, maps of adhesion force (row 2) and spring constant (row 3) revealed biochemical and biophysical heterogeneities of the cell wall during cell division. It is interesting to note that the septal furrow regions (highlighted by curves in **Fig. 3c1**, **3f1**) and the newly formed poles of daughter cells (green arrows or curve highlighted in **Fig. 3d**, **3g**) possess significantly lower *F*ad, k_b and E_{cell} than the rest of the cell wall, which should be closely correlated with alterations in the viscoelasticity behaviours of dividing *M. JLS*, and in return could be exploited to facilitate the separation of two newly formed offspring. In addition, we also noticed that *M. JLS* has an adhesion force similar to that of other mycobacterium species, such as *M. bovis BCG* (~3 nN) [3], which may be due to their similar cell wall structures.

To *in situ* track ethambutol (EMB)-induced cell wall destructions and resulting nanomechanical changes of living *M. JLS*, consecutive observations and measurements were conducted at the EMB concentration of 10 µg/ml (**Fig. 4**). Mechanical maps showed that significant down-regulations in adhesion force and elasticity were accompanied with cell wall destructions (**Fig. 4**), as confirmed by further statistical analysis (**Figs. 4j-4l**). For example, with a 10 µg/ml EMB treatment at the moment of visible cell wall destruction (**Fig. 4d→4e**), adhesion force of the cell wall surface decreased from 2.575±0.107 nN to 0.679±0.030 nN, cell spring constant decreased from 0.264±0.005 N/m to 0.104±0.002 N/m, and Young's modulus decreased from 19.000±2.213 MPa to 5.144±0.612

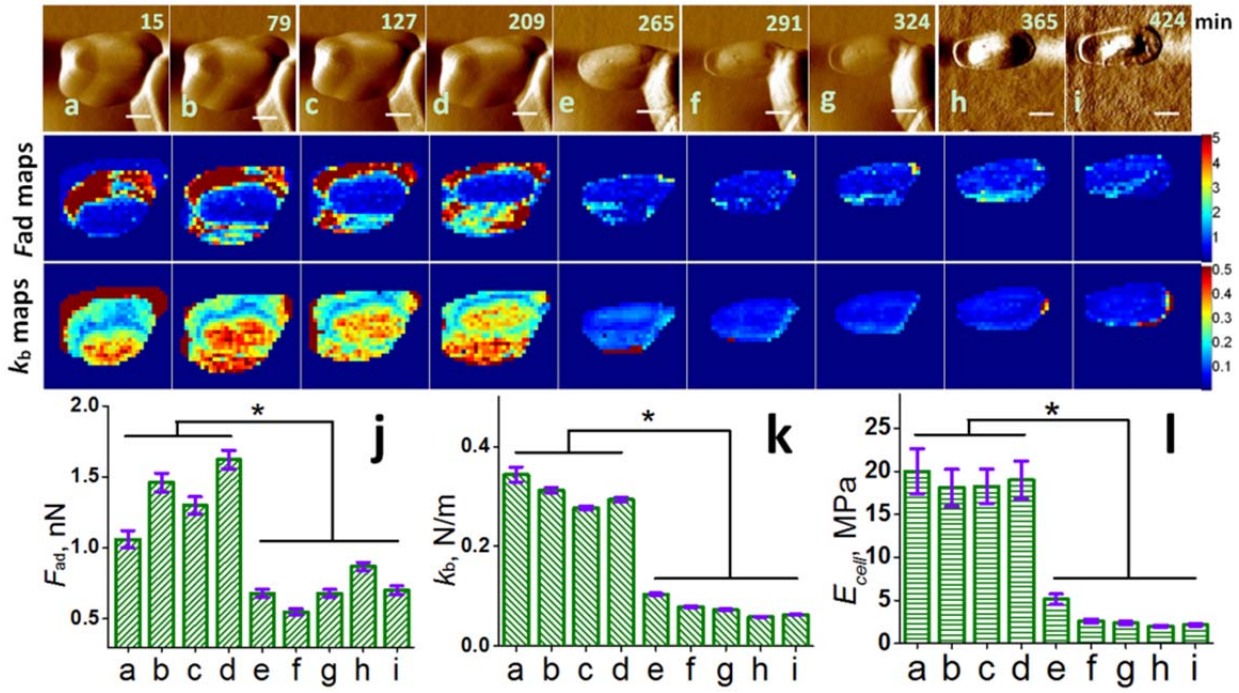

Figure 4: *In situ* consecutive observations and measurements of *M. JLS*-EMB (10 µg/ml) interaction acquired using contact mode AFM in culture medium. The observations of EMB induced cell wall destruction of *M. JLS* are shown in the first row **(a-i)**, and the maps of *F*ad and k_b acquired at each time point are correspondingly displayed under the images (the second and third rows, respectively). **(j-l)** Statistical comparison of F_{ad}, k_b, and E_{cell} over interaction time of *M.JLS*-EMB; a significant difference before and after cell wall collapse can be seen. * $P< 0.01$. Each time point has a different datum point 'n' that ranges from ~300 to ~700. Scale bar: 500 nm.

MPa. Notably, adhesion force maps indicated that the cell edge possesses a higher adhesion force (**Fig. 4**), which should be ascribed to the convolution effects of tip geometry and the cell shape itself, as previously discussed [10], and such data were thus excluded from statistical analyses.

4 CONCLUSION

In the present study we achieved direct consecutive observation of dividing *mycobacterium*, including emergence of the 'contractile ring', formation of the septal furrow, and dynamic processes of cell division. Further, time-dependent EMB-induced dynamic alterations in mycobacterial cell wall architectures and mechanical behaviours were evaluated at single cell level. This work not only demonstrated the successful application of AFM for simultaneous topographical visualizations and nanomechanical measurements of single dividing cells, but it also provided new opportunities to further interpret the mechanism of drug–living cell dynamic interaction at the single-cell level.

5 REFERENCES

1. L. C. O. Lazzarini, S. M. Spindola, H. Bang, A. L. Gibson, S. Weisenberg, W. D. Carvalho, C. J. Augusto, R. C. Huard, A. L. Kritski and J. L. Ho, *J. Clin. Microbiol.*, 2008, **46**, 2175-2183.
2. D. Kaur, M. E. Guerin, H. Skovierova, P. J. Brennan and M. Jackson, *Adv Appl Microbiol*, 2009, **69**, 23-78.
3. D. Alsteens, C. Verbelen, E. Dague, D. Raze, A. R. Baulard and Y. F. Dufrene, *Pflugers Arch.*, 2008, **456**, 117-125.
4. C. Verbelen, V. Dupres, F. D. Menozzi, D. Raze, A. R. Baulard, P. Hols and Y. F. Dufrene, *FEMS Microbiol. Lett.*, 2006, **264**, 192-197.
5. P. Parot, Y. F. Dufrene, P. Hinterdorfer, C. Le Grimellec, D. Navajas, J. L. Pellequer and S. Scheuring, *J. Mol. Recognit.*, 2007, **20**, 418-431.
6. Y. F. Dufrene, *Nat. Rev. Microbiol.*, 2008, **6**, 674-680.
7. C. D. Miller, K. Hall, Y. N. Liang, K. Nieman, D. Sorensen, B. Issa, A. J. Anderson and R. C. Sims, *Microb Ecol*, 2004, **48**, 230-238.
8. Y. Liang, D. R. Gardner, C. D. Miller, D. Chen, A. J. Anderson, B. C. Weimer and R. C. Sims, *Appl Environ Microbiol*, 2006, **72**, 7821-7828.
9. D. Lechner, S. Gibbons and F. Bucar, *Phytochem Lett*, 2008, **1**, 71-75.
10. Y. Z. Wu and A. Zhou, *Chem. Commun. (Camb)*, 2009, 7021-7023.